

DistributedEstimator: Distributed Training of Quantum Neural Networks via Circuit Cutting

Prabhjot Singh, Adel N. Toosi and Rajkumar Buyya

Quantum Cloud Computing and Distributed Systems (qCLOUDS) Lab

School of Computing and Information Systems

The University of Melbourne, Australia

Abstract—Circuit cutting decomposes a large quantum circuit into a collection of smaller subcircuits. The outputs of these subcircuits are then classically reconstructed to recover the original expectation values. While prior work characterises cutting overhead largely in terms of subcircuit counts and sampling complexity, its end-to-end impact on iterative, estimator-driven training pipelines remains insufficiently measured from a systems perspective. In this paper, we propose a cut-aware estimator execution pipeline that treats circuit cutting as a staged distributed workload and instruments each estimator query into partitioning, subexperiment generation, parallel execution, and classical reconstruction phases. Using logged runtime traces and learning outcomes on two binary classification workloads (Iris and MNIST), we quantify cutting overheads, scaling limits, and sensitivity to injected stragglers, and we evaluate whether accuracy and robustness are preserved under matched training budgets. Our measurements show that cutting introduces substantial end-to-end overheads that grow with the number of cuts, and that reconstruction constitutes a dominant fraction of per-query time, bounding achievable speed-up under increased parallelism. Despite these systems costs, test accuracy and robustness are preserved in the measured regimes, with configuration-dependent improvements observed in some cut settings. These results indicate that practical scaling of circuit cutting for learning workloads hinges on reducing and overlapping reconstruction and on scheduling policies that account for barrier-dominated critical paths.

I. INTRODUCTION

Hybrid quantum-classical workloads are increasingly shaped by a systems constraint rather than a purely algorithmic one: the circuits and training loops of practical interest frequently exceed the width, depth, or reliability envelope of near-term devices, while still requiring repeated expectation estimation in an interactive optimisation loop [1]–[3]. In this regime, execution is dominated by *estimator-heavy* pipelines that combine many short quantum jobs with non-trivial classical orchestration, aggregation, and optimiser feedback [4], [5]. As a result, the end-to-end performance of quantum machine learning (QML) and variational training is governed not only by circuit latency, but also by how effectively we schedule, parallelise, and reconstruct large collections of sub-tasks under heterogeneous runtimes [6]–[8].

Circuit cutting provides a principled mechanism to execute circuits that do not fit a target backend by decomposing them into smaller subcircuits that can be executed independently, followed by classical reconstruction of the desired quantity [9]–[12]. This transforms a single circuit evaluation into a

staged distributed workload: a fan-out of subcircuit executions, followed by a global reduction step that reconstructs the target expectation value (and, in learning settings, supports gradient estimation and optimiser updates). The methodological benefits of cutting are clear. The systems implications are less well characterised. Existing work typically reports overhead in terms of subcircuit counts, sampling complexity, or asymptotic reconstruction cost [10], [12], [13], which is informative for feasibility but does not directly answer the operational question that governs scaling: *where does wall-clock time go when we actually run the pipeline in parallel?*

Problems and limitations. We identify three practical limitations that motivate our study.

P1: Overhead attribution is under-specified. Cutting introduces additional compilation steps, subcircuit materialisation, task dispatch, and classical reconstruction. These costs are often treated as secondary to quantum execution or summarised coarsely. Without instrumentation that attributes time across stages, it is difficult to determine whether observed slowdowns are intrinsic to the cutting method or artefacts of the execution runtime and scheduling policy.

P2: Reconstruction can dominate the critical path. The decomposition induced by cutting increases parallelism in subcircuit execution but also concentrates work in a reconstruction stage that aggregates results across many subcircuits. In distributed computing, analogous reduction phases are known to bound scalability even when upstream work parallelises well [6], [8]. Without measuring the reconstruction share of end-to-end runtime under scale-out, it is unclear whether additional workers reduce total time or merely shift idle time upstream.

P3: Training dynamics, accuracy, and robustness must be assessed end-to-end. Circuit cutting aims to preserve the target computation, but in learning pipelines the optimiser observes finite-sample estimators and potentially different noise profiles. Small changes in estimator variance or evaluation ordering can alter optimisation trajectories, and practical effects may only appear when integrating cutting with training [2]–[4]. Moreover, if the resulting models are to be meaningful, we must check not only predictive accuracy but also robustness behaviour under the same training protocol [14], [15].

These limitations are systems problems as much as they are quantum problems: they concern staging, scheduling, aggregation, and the interaction between distributed execution and iterative optimisation.

Research questions. We therefore structure the paper around the following research questions (RQs), designed to be answered by measured runtime logs and training traces rather than by asymptotic arguments:

- 1) *RQ1 (Cutting overhead):* What additional end-to-end overheads are introduced by circuit cutting compared to an uncut execution baseline, and how do these overheads scale with the degree of parallelism?
- 2) *RQ2 (Scalability bottlenecks):* Which pipeline stages bound scaling under parallel execution, and under what conditions does classical reconstruction become the dominant contributor to wall-clock time?
- 3) *RQ3 (Scheduling policy and staggering):* How do execution policies that stagger or otherwise reshape subcircuit dispatch affect throughput, straggler sensitivity, and overall time-to-solution?
- 4) *RQ4 (Accuracy and training behaviour):* Does cutting preserve task accuracy under identical training protocols, and can the induced estimator and scheduling characteristics measurably influence training stability (e.g., convergence behaviour) relative to the uncut baseline?
- 5) *RQ5 (Robustness):* How does circuit cutting affect robustness metrics under the same evaluation regime, and are observed changes attributable to estimator effects rather than to changes in model definition?

We emphasise that each RQ is framed to admit an unambiguous operationalisation in our measurements: we measure stage-level durations, derive scaling trends and bottleneck shares from those measurements, and evaluate accuracy and robustness outcomes from recorded training and evaluation traces.

Approach overview. To answer these questions, we design an estimator-based execution pipeline that makes cutting explicit as a staged distributed workload. At a high level, our system: (i) generates a cut plan and the associated family of subcircuits required by the chosen cutting method [10], [12], (ii) executes subcircuits as independent tasks on a distributed runtime, (iii) reconstructs target estimates via a dedicated aggregation phase, and (iv) feeds reconstructed estimates into an iterative training loop. Critically, we instrument each stage to produce time-stamped records of compilation, dispatch, execution, and reconstruction, enabling stage-level attribution under varying degrees of parallelism and scheduling policies.

Our evaluation methodology is correspondingly systems-driven. We do not assume that more parallel workers yield proportional speed-ups; instead, we quantify where the critical path shifts as we scale out, using the same experimental protocol across baseline (no cut) and cut variants. For RQ3, we implement and compare scheduling policies that intentionally reshape concurrency (including staggering) to reduce contention and mitigate stragglers, drawing on established insights from heterogeneous cluster scheduling and tail-latency mitigation [7], [16]. For RQ4–RQ5, we couple the runtime measurements with training logs to ensure that any performance improvements are not purchased by silent degradation

in model outcomes.

Contributions. Our main contributions are as follows:

- *A measurement-driven formulation of circuit cutting as a distributed staged pipeline,* with instrumentation that attributes end-to-end time across cutting, subcircuit execution, reconstruction, and training.
- *An empirical scalability analysis grounded in stage-level logs,* enabling bottleneck identification and explaining when additional parallelism does not translate into reduced wall-clock time due to aggregation and coordination effects.
- *A study of scheduling policies for cutting workloads,* including staggered dispatch strategies, evaluated through measured throughput and tail behaviour rather than assumed ideal parallelism.
- *An end-to-end assessment of learning outcomes,* reporting accuracy and robustness under consistent training protocols to distinguish performance gains from changes in optimisation behaviour.

Together, these contributions establish a systems-level understanding of the performance trade-offs introduced by circuit cutting in estimator-heavy training pipelines, and provide a reproducible basis for reasoning about overheads, bottlenecks, and outcome preservation under distributed execution.

II. BACKGROUND AND RELATED WORK

In this section, we summarise the technical background required to interpret our system design and measurements, and we position our work against the most relevant literature on circuit cutting, hybrid quantum–classical execution, and distributed performance bottlenecks.

A. Background

Hybrid quantum–classical workloads and variational training. Near-term quantum devices operate in the *Noisy Intermediate-Scale Quantum* (NISQ) regime, where limited qubit counts and noise constrain executable circuit width and depth [1]. A prevalent approach in this regime is the *variational quantum algorithm* (VQA), which couples a parameterised quantum circuit with a classical optimiser [2], [17]–[19]. This hybrid loop underpins much of quantum machine learning (QML), including parameterised quantum models [20], [21] and kernel-style feature maps [22]. For learning tasks with classical data, practical feasibility often depends as much on data access patterns and estimator variance as on the expressivity of the quantum model [23].

From a systems perspective, VQA training is dominated by repeated evaluation of expectation values and (often) gradients. Analytic gradient schemes such as the parameter-shift rule are attractive because they avoid finite-difference instability but still multiply circuit evaluations [4]. In addition, the optimisation landscape can be problematic (e.g., barren plateaus), which can increase the number of training iterations and amplify any per-iteration overheads [2], [24]. Consequently, end-to-end runtime is governed by a composition of quantum execution latency, the number of circuit evaluations

required by the optimiser, and classical orchestration and post-processing costs [1], [2].

Noise and sampling error further complicate this picture. Error mitigation can improve estimator accuracy without full fault tolerance, but it typically adds additional circuit executions and classical processing steps [3], [5]. The resulting workload is therefore *estimator-heavy*: it comprises large numbers of small quantum jobs plus non-trivial classical aggregation, often executed in an interactive loop [2], [3].

Estimator abstractions and execution models. Most near-term applications consume quantum hardware through an expectation-value interface: a circuit (or parameterised circuit) together with one or more observables yields an estimate with finite-sample variance. Modern software stacks expose this explicitly. For example, the Qiskit architecture and workflow are documented in an authoritative, citable form [25], and its *Estimator* and *Sampler* primitives formalise expectation and sampling as first-class execution units [26]. Similarly, differentiable programming toolchains integrate quantum evaluations into classical automatic differentiation and optimisation (e.g., plugin-based device backends) [27], [28].

These abstractions are convenient, but they also make performance failure modes more predictable: (i) the number of circuit evaluations grows with the estimator variance and the optimiser’s query complexity, (ii) the aggregation step becomes unavoidable for training and reconstruction, and (iii) the effective critical path may be dominated by orchestration and reduction rather than by raw quantum execution [3]–[5]. Our paper explicitly treats this as a distributed systems problem: we measure and attribute overheads across pipeline stages rather than assuming “quantum time” is the only knob that matters.

Circuit cutting and classical reconstruction. Circuit cutting (often discussed under the umbrella of *circuit knitting*) decomposes a circuit that does not fit a target backend into a collection of smaller subcircuits that do, at the cost of classical reconstruction and increased sampling complexity [9]–[11]. The core trade-off is structural: cutting reduces spatial requirements (qubits) while increasing the number of executions and the weight of post-processing [9], [10].

Practical toolflows typically involve three stages. First, a compiler or optimiser chooses cut locations and a decomposition strategy [10], [12]. Second, a set of subcircuits (often many variants induced by the decomposition) are executed and measured [10], [13]. Third, a classical reconstruction procedure aggregates sub-results into an estimate of the target quantity (e.g., an expectation value) [10]–[12]. Recent work shows that allowing classical communication between sub-components can reduce overhead constants in certain settings [11], and that alternative cutting schemes based on randomised measurements provide different accuracy–cost trade-offs [13].

Importantly for systems evaluation, cutting turns a single “large” circuit evaluation into a *task graph* with (often) substantial fan-out followed by a global aggregation. This introduces obvious bottleneck candidates: scheduling overhead,

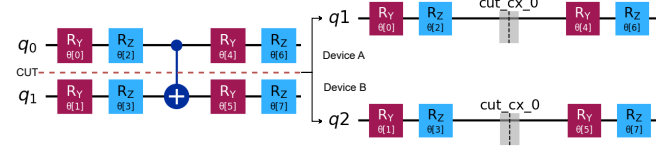


Fig. 1: Inpedependent subcircuits generated by cutting circuit.

straggler sensitivity across large job sets, and a potentially heavy reduction (reconstruction) stage [10], [12]. These are precisely the failure modes we can only resolve by measured profiling rather than by asymptotic overhead counts alone.

Distributed execution, stragglers, and staged pipelines.

Distributed systems research has repeatedly shown that scalability is frequently capped by coordination and stragglers rather than by idealised parallel work. MapReduce made this explicit, and speculative execution policies (e.g., LATE) were introduced specifically to mitigate heterogeneous task runtimes [6], [7]. In-memory dataflow systems and cluster computing abstractions (e.g., resilient distributed datasets) improved throughput for iterative workloads but still expose similar scheduling and reduction bottlenecks [29]. General-purpose task-graph engines such as Ray provide dynamic execution with task/actor abstractions that are well-suited to large ensembles of fine-grained jobs [16], while Python-native schedulers (e.g., Dask) emphasise blocked algorithms and dynamic task scheduling for scientific workloads [30].

Distributed machine learning (ML) provides a particularly relevant analogue. Parameter-server designs and consistency models were developed to manage synchronisation and straggler effects in synchronous and bounded-asynchrony regimes [31], [32]. Lock-free and asynchronous update schemes can improve throughput when assumptions (e.g., sparsity) hold, but they trade determinism for performance [33]. Data-parallel training commonly relies on collective communication (e.g., all-reduce), where communication structure and hierarchy-aware decomposition directly impact scaling [8], [34]. Even when compute parallelises cleanly, aggregation phases can dominate at scale [8], [35]. Work stealing provides a classic lens for understanding load balancing under irregular parallelism [36].

Circuit cutting produces a staged pipeline with the same fundamental shape: embarrassingly parallel subcircuit execution followed by a global reconstruction. Therefore, the relevant question is not whether parallelism exists, but whether reconstruction and coordination costs dominate the critical path as we scale out [7], [8], [10]. Our evaluation is designed to quantify this boundary empirically.

B. Related Work

We organise related work into (i) circuit cutting methods and their overhead models, (ii) hybrid software stacks and execution interfaces, and (iii) distributed systems techniques for scaling estimator-heavy workloads.

Circuit cutting methods, overheads, and optimisation targets. Peng et al. [9] introduced a cluster simulation view that makes explicit how limited quantum memory can be traded for exponential overhead in structural parameters, motivating decomposition as a route to execute circuits beyond device width. CutQC [10] provided an end-to-end toolflow that automates cut selection and reconstruction, and it documented that classical post-processing and the number of required subcircuits can grow rapidly with number and type of cuts. Subsequent work studied overhead reductions via classical communication [11] and via randomised measurement strategies that change the sampling profile [13]. More recently, optimisation objective itself has been formalised: Harrow et al. [12] study optimality notions for cuts and provide bounds and constructions that clarify when overhead is unavoidable.

A complementary line of work investigates multi-processor or modular execution, including demonstrations combining multiple quantum processors with real-time classical coordination, alongside circuit cutting and dynamic control flow [37]. Industrial toolchains also explore serverless and managed execution environments for cutting workloads, reflecting an implicit acknowledgement that orchestration and classical processing are first-order concerns [38]–[40].

However, much of the circuit-cutting literature reports overhead primarily in terms of *counts* (numbers of subcircuits, asymptotic reconstruction complexity, sampling blow-up) rather than in terms of *measured* end-to-end time attribution on a distributed runtime. This limits our ability to understand when reconstruction becomes the bottleneck, how stragglers shape tail latency, and whether scheduling policies (e.g., staggering) materially affect throughput in practice.

Hybrid stacks and estimator-oriented interfaces. The software ecosystem for hybrid execution has matured significantly. Qiskit [25] provides a widely used compilation and execution stack, and its design decisions and core components have been documented in a citable form suitable for systems and methodology discussion. Qiskit’s primitives [26] make expectation-value estimation and sampling explicit in the programming model. PennyLane [27] and TensorFlow Quantum [28] integrate quantum circuit evaluation into differentiable programming and ML workflows, providing interfaces that naturally generate estimator-heavy execution patterns. These stacks enable rapid prototyping, but they generally do not provide a systems-level analysis of distributed bottlenecks for cutting-plus-training pipelines; instead, performance is often reported at level of circuit runtime or simulator throughput [27], [28].

On the algorithmic side, error mitigation and hybrid methods emphasise that practical near-term execution requires additional classical processing and repeated circuit evaluations [3], [5]. VQA surveys highlight that measurement cost and optimiser query complexity are central constraints [2], [18]. Yet, the interaction between these algorithmic requirements and distributed execution policies is typically left implicit. Our work treats this interaction as primary object of measurement.

Distributed ML and straggler-aware scheduling. Dis-

tributed ML provides established methods and cautionary lessons. Parameter-server architectures and bounded-staleness models reduce idle time under heterogeneity while maintaining correctness guarantees under controlled delay [31], [32]. Speculative execution strategies mitigate tail latency in large job sets [7], and general task-graph engines scale fine-grained workloads by separating control and data planes [16]. Communication libraries and all-reduce decompositions show that collective aggregation can dominate and that topology-aware design is critical [8], [34]. Large-batch scaling studies reinforce that synchronisation and communication, not just computation, control speed-up at scale [35].

Robustness and stability further motivate careful evaluation. Classical adversarial robustness work demonstrates that training dynamics and optimisation procedures materially affect robustness properties [14], [15], [41], [42]. In estimator-heavy quantum-classical training, analogous concerns arise from sampling noise, estimator variance, and distribution shifts induced by decomposition choices, which can alter optimisation trajectories even when the target function is theoretically preserved [2]–[4]. Existing work rarely connects these robustness/stability questions to the systems bottlenecks introduced by cutting and reconstruction.

Summary and gap. Prior work establishes that circuit cutting can extend executable circuit sizes [9], [10], and it clarifies key overhead trade-offs and potential reductions [11]–[13]. In parallel, hybrid software stacks expose estimator-oriented execution models [25]–[28], while distributed systems research provides mature techniques for reasoning about stragglers and aggregation bottlenecks [6]–[8], [31]. What remains underexplored is a measurement-driven, system-level account of how cutting transforms end-to-end training into a staged distributed pipeline, when reconstruction dominates, and which execution policies materially improve throughput without degrading accuracy or robustness. Our paper addresses this gap by instrumenting and attributing costs across cutting, subcircuit execution, reconstruction, and training dynamics under controlled distributed execution.

III. SYSTEM MODEL AND PROBLEM FORMULATION

In this section, we formalise the estimator-driven, cut-aware training pipeline as a staged distributed computation and define measurable performance and outcome quantities aligned with our research questions (RQ1–RQ5).

End-to-end pipeline model. Figure 2 shows the pipeline we evaluate. A classical dataset is preprocessed and supplied to a training loop. Each iteration evaluates a quantum neural network (QNN) forward pass and associated loss, and updates parameters via a classical optimiser. The forward pass is implemented via expectation estimation queries of the form $(C(\theta, x), O)$, where C is a parameterised circuit instantiated at parameters θ and input x , and O is the observable (or set of observables) required to compute model outputs and loss [2], [4].

When circuit cutting is enabled, the estimator query is expanded into a set of subexperiments that can be executed

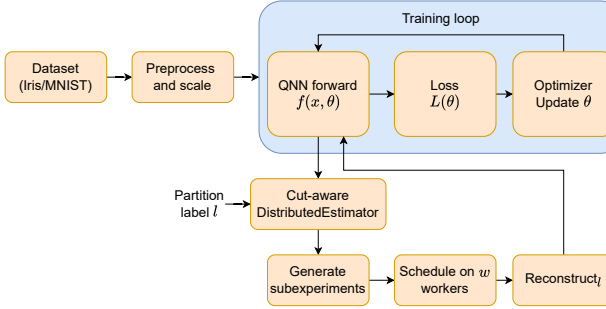


Fig. 2: Training pipeline with a cut-aware distributed estimator. Circuit cutting expands each estimator query in the QNN forward/gradient evaluation into parallel subexperiments followed by classical reconstruction.

independently, followed by a classical reconstruction step that returns the estimate to the training loop [9], [10], [12]. This transformation is central to our study because it introduces (i) additional overheads beyond baseline execution (RQ1), (ii) a reconstruction barrier that can dominate the critical path under scale-out (RQ2), and (iii) scheduling degrees of freedom, including staggering, that affect straggler sensitivity and throughput (RQ3). The same transformation may also affect learning dynamics through estimator variance and evaluation order, which we examine through accuracy and robustness outcomes (RQ4–RQ5).

Cut-aware estimator query model. For a single query instance $(C(\theta, x), O)$, circuit cutting produces a partition labelled by ℓ and yields subcircuits and subobservables. The resulting execution requires a finite set of concrete subexperiments $\mathcal{E} = \{e_k\}_{k=1}^K$ and reconstruction coefficients α determined by the cutting scheme and partition [10], [12]. Each e_k is executed with a fixed shot count S , producing a classical summary r_k (e.g., outcome counts). Reconstruction aggregates $\mathcal{R} = \{r_k\}$ into an estimate \hat{y} of the target expectation value.

This induces a staged cost decomposition for each query instance:

$$T_{\text{total}} = T_{\text{part}} + T_{\text{gen}} + T_{\text{exec}} + T_{\text{rec}}, \quad (1)$$

where:

- T_{part} is circuit/observable partitioning time (including cut planning and partition materialisation);
- T_{gen} is subexperiment generation time (including basis variants and reconstruction coefficients);
- T_{exec} is parallel execution time of \mathcal{E} on a worker pool;
- T_{rec} is classical reconstruction time.

Eq. (1) provides the measurement backbone for RQ1 and RQ2: we report each component as a measured quantity and study how their shares evolve with the degree of parallelism.

Execution, stragglers and scheduling. We model subexperiment execution as a set of independent tasks scheduled on w workers, followed by a reconstruction barrier. Figure 3 captures this per-query expansion and the straggler sensitivity introduced by the barrier. Let t_k denote the service time for

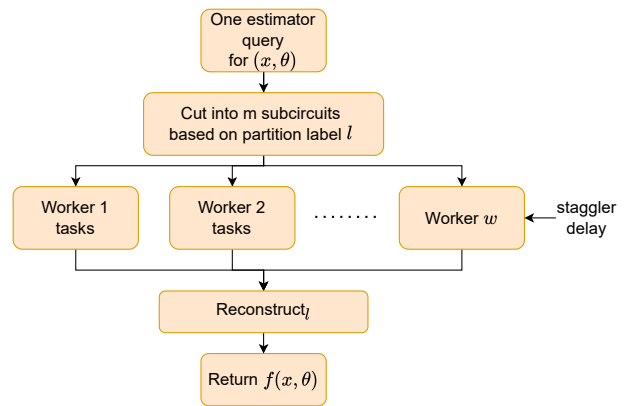


Fig. 3: Per-query expansion under circuit cutting. Subexperiments execute across w workers; reconstruction forms a barrier and is sensitive to straggler delays.

subexperiment e_k (including dispatch and backend runtime). Under a work-conserving policy, the realised parallel time is governed by load balance and tail effects and can be expressed as:

$$T_{\text{exec}} \approx \max_{i \in \{1, \dots, w\}} \sum_{k \in \mathcal{A}(i)} t_k, \quad (2)$$

where $\mathcal{A}(i)$ is the assignment of subexperiments to worker i . This form makes explicit why speed-up can saturate even when the task set is abundant: T_{exec} is bounded by the slowest worker, and T_{rec} is a serial reduction that must wait for all results, mirroring classical bottlenecks in staged distributed computations [6], [7].

To study straggler sensitivity repeatedly, we allow an optional synthetic delay process at the task level. Each subexperiment independently incurs an injected delay Δ with probability p , yielding $t'_k = t_k + 1\{u_k < p\}\Delta$ for $u_k \sim \text{Uniform}(0, 1)$. We use this mechanism strictly as an experimental control to stress the tail of Eq. (2) and to evaluate whether scheduling choices (including staggering) reduce end-to-end time-to-solution under heterogeneity [7].

Problem definition. We consider a fixed training protocol (dataset split, optimiser, stopping criterion) and a fixed per-subexperiment shot budget S . For a given configuration (cut plan ℓ , worker pool size w , scheduling policy π , and optional straggler parameters), our primary systems objective is to minimise *time-to-solution* while preserving learning outcomes:

$$\min_{\pi \in \Pi} \mathbb{E}[T_{\text{total}}] \quad \text{s.t. accuracy and robustness constraints.} \quad (3)$$

We operationalise this objective through:

- *Measured:* $T_{\text{part}}, T_{\text{gen}}, T_{\text{exec}}, T_{\text{rec}}, T_{\text{total}}$ per query instance (and their aggregation over training);
- *Derived:* stage shares (e.g., $T_{\text{rec}}/T_{\text{total}}$), scaling curves as a function of w , and bottleneck attribution via changes in dominant stage across configurations;

Algorithm 1: Instrumented cut-aware estimator for one query instance

Require: Circuit $C(\theta, x)$, observable O , partition label ℓ , shots S , workers w , scheduling policy π

- 1: Initialise timers and metadata record
- 2: **Partition:** $(\{C_i\}, \{O_i\}, \mathcal{B}) \leftarrow \text{PartitionProblem}(C, O, \ell)$
- 3: **Generate:** $(\mathcal{E}, \alpha) \leftarrow \text{GenerateSubexperiments}(\{C_i\}, \{O_i\}, S)$
- 4: **Execute:** $\mathcal{R} \leftarrow \text{ExecuteTasks}(\mathcal{E}, w, \pi)$
- 5: **Reconstruct:** $\hat{y} \leftarrow \text{Reconstruct}(\mathcal{R}, \alpha, \{O_i\}, O)$
- 6: Log $(T_{\text{part}}, T_{\text{gen}}, T_{\text{exec}}, T_{\text{rec}}, T_{\text{total}})$ and metadata to JSONL
- 7: **return** \hat{y}

- *Observed:* training outcomes (accuracy) and robustness metrics computed under a consistent evaluation regime.

This mapping directly supports RQ1–RQ5: overhead and scaling are answered by timing breakdowns and their evolution with w ; the existence of a reconstruction bottleneck is established by measured dominance of T_{rec} and the saturation of speed-up; the impact of staggering is established by changes in T_{exec} tail behaviour and T_{total} ; and outcome preservation is established by measured accuracy and robustness under unchanged training and evaluation procedures.

IV. METHODOLOGY

In this section, we describe how we implement the cut-aware distributed estimator, how we instrument stage-level timings and outcomes, and how we configure scheduling policies and straggler controls to answer RQ1–RQ5.

Cut-aware distributed estimator. Our estimator backend implements a cut-aware execution path that transforms each query instance $(C(\theta, x), O)$ into a set of subexperiments and a reconstruction plan. Concretely, for each query instance we: (i) partition the problem according to a partition label ℓ , (ii) generate the concrete subexperiments \mathcal{E} and reconstruction coefficients α , (iii) execute \mathcal{E} across a worker pool of size w , (iv) reconstruct the target estimate \hat{y} , (v) return \hat{y} to the training loop.

The key methodological choice is to treat this as a *staged* pipeline and to instrument each stage individually. This allows us to attribute overheads introduced by cutting (RQ1) and to identify scaling limits caused by reconstruction and coordination (RQ2) without conflating them with training-loop compute.

Algorithm 1 summarises the per-query logic. The algorithm is intentionally phrased to align with logged quantities and the timing decomposition in Eq. (1).

Scheduling policies and staggering. We evaluate execution policies that differ only in how they submit and allocate the task set \mathcal{E} to a bounded worker pool of size w . The baseline policy is eager submission with a work-conserving runtime. To evaluate staggering (RQ3), we introduce a dispatch control

Algorithm 2: Task dispatch with optional staggering

Require: Task set \mathcal{E} , workers w , policy π (batch size B , inter-batch delay δ , ordering rule)

- 1: Order tasks \mathcal{E} according to π (e.g., FIFO, grouped by label)
- 2: Partition ordered tasks into batches $\{\mathcal{E}^{(b)}\}$ of size B (or one batch if eager)
- 3: **for** each batch $\mathcal{E}^{(b)}$ **do**
- 4: Submit all $e_k \in \mathcal{E}^{(b)}$ to the worker pool; collect futures
- 5: **if** $\delta > 0$ **then**
- 6: Sleep for δ
- 7: **end if**
- 8: **end for**
- 9: Wait for all tasks; return results \mathcal{R}

that spaces submissions or groups tasks (e.g., by partition label or by fixed-size batches) and enforces a bounded inter-batch delay. We treat staggering as a scheduling intervention that can reduce transient contention and mitigate tail effects in T_{exec} , but we do not assume improvement: its impact is assessed solely through measured T_{exec} distributions and end-to-end T_{total} .

Algorithm 2 gives a generic dispatch routine that captures both eager submission and staggered submission as special cases via the policy π .

Straggler control. When enabled, synthetic straggler injection is applied at task execution time. This allows us to stress the barrier sensitivity in Fig. 3 and evaluate whether staggering or alternative ordering reduces end-to-end latency by reshaping the tail of T_{exec} (RQ3). We log injected delays alongside per-stage timings to ensure that straggler effects are explicitly traceable in subsequent analysis.

Instrumentation and outcome tracking. For each estimator query, we emit a JSONL record containing: (i) query structure (e.g., number of subexperiments K , shots S), (ii) configuration (partition label ℓ , worker pool size w , scheduling policy identifier, straggler parameters when enabled), and (iii) measured stage timings consistent with Eq. (1). At the training level, we log loss traces, optimiser steps, and evaluation metrics.

This instrumentation supports:

- *RQ1:* compare baseline vs cut variants via differences in $(T_{\text{part}} + T_{\text{gen}} + T_{\text{rec}})$ and changes in T_{exec} under matched shot budgets;
- *RQ2:* attribute scaling saturation to dominant stage shares and reconstruction-barrier behaviour;
- *RQ3:* quantify the effect of staggering and ordering on T_{exec} tail behaviour and end-to-end T_{total} ;
- *RQ4–RQ5:* evaluate whether accuracy and robustness metrics are preserved under identical training and evaluation procedures, and relate any changes to measured estimator-stage behaviour rather than untracked confounders.

V. EVALUATION

We evaluate the proposed cut-aware estimator pipeline using instrumented execution traces to quantify end-to-end overheads, scaling behaviour, sensitivity to injected stragglers, and learning outcomes (accuracy and robustness). All claims in this section are grounded in measured quantities recorded in the run-level records, estimator-call summaries, and robustness traces.

A. Experimental Setup

Software stack. All experiments are implemented in Python. Quantum circuits are constructed in Qiskit [43] and executed using the Aer primitive interface (SamplerV2/AerSampler, depending on installed *qiskit-aer* version). Circuit cutting is implemented with *qiskit-addon-cutting* [44] via the standard decomposition workflow (problem partitioning, generation of cutting experiments, and classical reconstruction). The learning pipeline uses *qiskit-machine-learning* (EstimatorQNN and TorchConnector [45]) and PyTorch for optimisation; MNIST [46] data handling uses Torchvision, and Iris preprocessing uses scikit-learn. The distributed execution model is implemented via a bounded worker pool (thread-based in our current implementation), with the worker count logged as *subexp_workers* (MNIST) or *max_subexp_workers* (Iris).

Model circuits: feature map and ansatz. Across both workloads, we instantiate a parameterised quantum circuit as the composition of a *ZFeatureMap* followed by a *RealAmplitudes* ansatz with one repetition (*reps*=1). For Iris, the observable is the tensor-product Pauli-Z operator $Z^{\otimes n}$, implemented as a *SparsePauliOp* with n qubits, yielding an expectation-value classifier output.

Workloads and training budgets. We consider two binary classification tasks: *iris_binary_pm1* and *mnist_binary*. We enforce matched comparisons within each dataset by fixing the estimator shot budget (1024 shots per (sub)experiment) and by restricting comparisons to runs executed under the same training budget and straggler configuration. For the clean (non-straggler) setting, we report results using the longest training budgets available for each dataset (Iris: *maxiter* = 60; MNIST: 10 epochs), with *straggler_delay_s*=0.0. For scaling analysis, we use shorter budgets (Iris: *maxiter* = 10; MNIST: 5 epochs), again with *straggler_delay_s*=0.0, to match the worker-count sweeps used in our scaling experiments. For straggler sensitivity, we inject delays of *straggler_delay_s*=0.1; these experiments use Iris with *maxiter* = 10 and MNIST with 3 epochs at 8 workers.

Cut descriptors used in plots. In all bar plots, colours indicate the cut setting: blue denotes *NO_CUT*, orange denotes one cut, green denotes two cuts, and red denotes three cuts.

Logging and derived metrics. We instrument each run to record end-to-end training time and test accuracy, stage-level timings (subexperiment execution and classical reconstruction), and robustness traces under injected Gaussian and FGSM perturbations. From these measurements, we report total training time as well as the fraction of time spent in

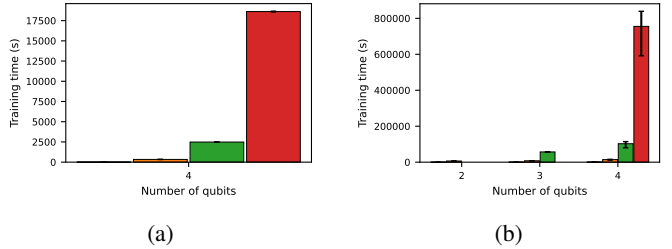


Fig. 4: RQ1: End-to-end training time under clean execution. Left: Iris (*maxiter* = 60). Right: MNIST (10 epochs).

TABLE I: RQ2: Reconstruction share from estimator-call summaries under clean execution (*straggler_delay_s*=0.0).

#cuts	<i>n</i>	median $T_{\text{Rec}}/T_{\text{total}}$	p95 $T_{\text{Rec}}/T_{\text{total}}$
1	41	0.430	0.474
2	28	0.489	0.533
3	5	0.530	0.580

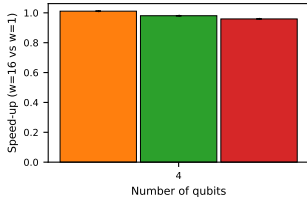
reconstruction versus subexperiment execution. When reporting scaling or straggler sensitivity as ratios, we compute ratios only between runs that match dataset, seed, model configuration, and cut label.

B. Results and Analysis

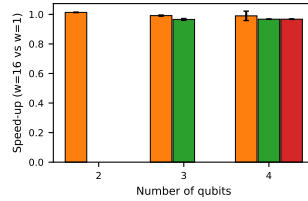
RQ1. Figure 4 reports end-to-end training time under the clean setting with the maximum training budgets available in our evaluation (Iris: *maxiter* = 60; MNIST: 10 epochs; *straggler_delay_s*=0.0 for both). Across both datasets, training time increases sharply with the number of cuts at fixed qubit descriptor, consistent with the fact that circuit cutting expands each estimator query into a larger collection of subexperiments and introduces a non-trivial reconstruction phase. Importantly, the effect is not a small constant surcharge: the growth is configuration-dependent and increases with cut count, which is consistent with a workload expansion rather than a fixed per-iteration overhead.

RQ2. We address scaling in two complementary ways. First, Figure 5 reports speed-up from increasing parallelism, defined as the ratio of training time at 1 worker to training time at 16 workers, computed only for matched seed and configuration pairs. For MNIST (5 epochs, clean), the observed speed-ups are close to 1 and frequently below 1, indicating that additional workers do not translate into proportional reductions in time-to-solution. Iris shows the same qualitative behaviour under *maxiter* = 10 for the configurations present at both 1 and 16 workers. Second, Table I quantifies the reconstruction share measured directly from estimator-call summaries: $T_{\text{rec}}/T_{\text{total}}$. Reconstruction accounts for a substantial fraction of estimator time and increases with cut count, directly supporting the interpretation that the reconstruction barrier bounds achievable speed-up even when subexperiment execution is parallelised.

RQ3. Figure 6 reports sensitivity to injected stragglers at *straggler_delay_s*=0.1, using the ratio of training time at straggler rate p = 0.2 to that at p = 0.0, computed for matched

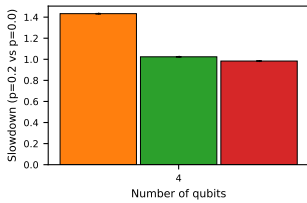


(a)

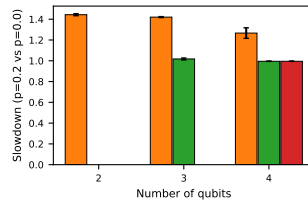


(b)

Fig. 5: RQ2: Scaling behaviour under clean execution. Bars report speed-up at 16 workers relative to 1 worker for matched pairs. Left: Iris ($maxiter = 10$). Right: MNIST (5 epochs).



(a)



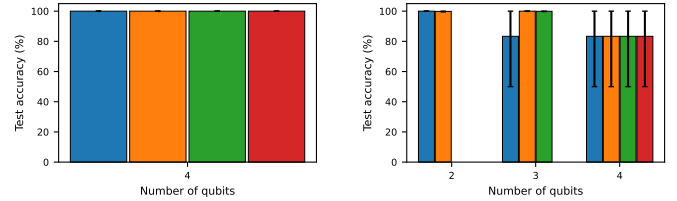
(b)

Fig. 6: RQ3: Straggler sensitivity at $straggler_delay_s=0.1$. Bars report slowdown at $p = 0.2$ relative to $p = 0.0$ for matched pairs (8 workers). Left: Iris ($maxiter = 10$). Right: MNIST (3 epochs).

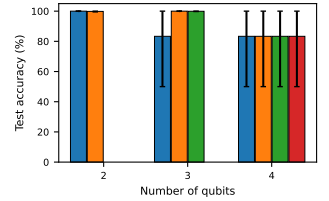
pairs. The resulting slowdowns vary across cut configurations. This indicates that straggler impact is not governed solely by the injected delay parameters, but by where the critical path lies: configurations dominated by reconstruction tend to exhibit smaller relative sensitivity to execution-side delays, whereas configurations with a larger execution share amplify tail latency more strongly.

RQ4. Figure 7 reports absolute test accuracy under the clean setting using the maximum training budgets available in our evaluation (Iris: $maxiter = 60$; MNIST: 10 epochs; $straggler_delay_s=0.0$). On Iris, all evaluated configurations achieve identical test accuracy, indicating that circuit cutting does not degrade final predictive performance in this setting. On MNIST, accuracy varies with qubit descriptor and random seed, but we do not observe systematic degradation as the cut count increases; instead, several cut configurations achieve accuracy comparable to or higher than the no-cut baseline under the same training budget. This behaviour is consistent with the fact that cutting changes the estimator workload and aggregation pattern, which can alter optimisation trajectories even when reconstruction is unbiased.

RQ5. We evaluate robustness using recorded perturbation traces under injected Gaussian noise and FGSM attacks. Figure 8 reports a single robustness summary per run, computed as the mean accuracy over non-zero perturbation magnitudes and averaged across Gaussian and FGSM traces when both are present. We use Iris with $maxiter = 60$ and MNIST with 10 epochs (both clean). For Iris, the robustness summary matches the clean accuracy across all evaluated configurations,

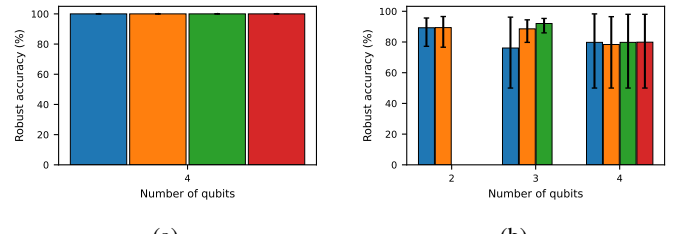


(a)

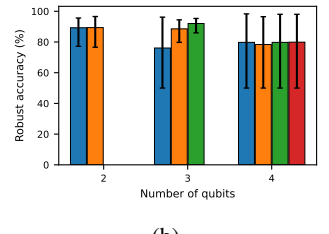


(b)

Fig. 7: RQ4: Absolute test accuracy under clean execution. Left: Iris ($maxiter = 60$). Right: MNIST (10 epochs).



(a)



(b)

Fig. 8: RQ5: Robustness summary under clean execution. Left: Iris ($maxiter = 60$). Right: MNIST (10 epochs).

indicating no measurable robustness degradation due to cutting under this evaluation. For MNIST, robustness varies across configurations; however, several cut configurations achieve robustness comparable to the baseline, and some achieve higher values within the logged runs. Given the limited number of seeds per configuration in the robustness traces, we report these effects as measured outcomes rather than universal guarantees.

VI. DISCUSSION AND FUTURE WORK

Our evaluation highlights that circuit cutting should be treated as a staged distributed workload rather than a purely algorithmic transformation. The central observation across RQ1–RQ3 is that, while cutting increases parallelisable work (subexperiment execution), it simultaneously introduces substantial non-parallel components (reconstruction and coordination) that dominate end-to-end performance in the measured regimes. This section consolidates these findings, explains the underlying mechanisms, and delineates concrete extensions that are directly motivated by the observed bottlenecks.

A. Discussion

Cutting overhead is dominated by workload expansion rather than planning. RQ1 shows that the dominant effect of cutting is not a small constant overhead from partitioning or experiment generation, but the expansion in the number of executable units and the associated aggregation cost. This aligns with the structure of cutting schemes: each additional cut increases the number of subexperiments and reconstruction terms, raising both the volume of executor work and the amount of intermediate state that must be reduced. The estimator-stage traces support this interpretation: partitioning

and generation remain comparatively small, whereas execution and reconstruction grow substantially with the cut count. Consequently, treating cutting as a one-off compilation step is misleading in a training pipeline; the transformation is paid repeatedly at estimator call granularity.

Reconstruction is a scaling limiter because it is a barrier on the critical path. RQ2 quantifies the reconstruction fraction and shows that reconstruction is a substantial share of per-query time and increases with cut count. This induces two scaling constraints. First, even if subexperiment execution scales ideally with workers, the serial reconstruction stage bounds achievable speed-up. Second, reconstruction acts as a barrier: the training loop does not progress until all required subexperiment results are available, which makes the pipeline sensitive to tail latency in upstream execution. These effects are visible in the scaling plots, where speed-up saturates and can degrade as worker counts increase. The implication is that parallelising subexperiment execution alone is insufficient for end-to-end gains unless reconstruction is reduced, overlapped, or distributed.

Straggler sensitivity depends on where time is spent. RQ3 indicates that injected stragglers can increase end-to-end time, but the magnitude of slowdown varies significantly across configurations. This is consistent with the staged model: when a configuration is already reconstruction-dominated, additional execution-side delays contribute a smaller fraction of the total wall-clock time; conversely, configurations with a larger execution share amplify tail latency more strongly. Therefore, scheduling interventions aimed solely at reducing execution variance (e.g., straggler mitigation policies) may produce limited benefit if reconstruction remains the bottleneck. This motivates scheduling designs that jointly consider (i) the distribution of subexperiment service times and (ii) the reconstruction workload and barrier placement.

Learning outcomes are preserved, and can be altered by estimator effects. RQ4 shows that accuracy is not systematically degraded by cutting under matched training budgets. In Iris, accuracy is invariant across evaluated configurations, whereas in MNIST the variance across seeds and configurations is more pronounced, and some cut configurations achieve higher accuracy. This does not imply that cutting is intrinsically beneficial for optimisation; rather, it underscores that cutting changes the estimator workload and aggregation characteristics, which can affect optimisation trajectories even when reconstruction is unbiased. In particular, changes in estimator variance, effective minibatch noise, and evaluation ordering can alter the stability of gradient-based training. These effects are configuration-dependent and therefore must be established empirically for each workload.

Robustness is not harmed in the measured regimes, but warrants careful attribution. RQ5 indicates that robustness metrics computed from the logged perturbation traces are comparable across cut and no-cut configurations in the measured settings, with improvements observed for some MNIST configurations. As with accuracy, we interpret these as measured outcomes rather than guarantees. Robustness can be influenced

by the same factors that affect training stability (noise scale, estimator variance, optimisation trajectory). Accordingly, robustness comparisons should be reported alongside the training budget, perturbation protocol, and any estimator configuration that affects sampling noise, and should not be inferred solely from functional equivalence of reconstruction.

B. Future Work

We frame future work as concrete, testable extensions motivated by the measured bottlenecks and limitations of our current prototype and experimental scope.

Distributed and incremental reconstruction. Given that reconstruction dominates in higher-cut regimes (RQ2), a natural direction is to redesign reconstruction as a distributed reduction rather than a monolithic post-processing step. Two promising approaches are: (i) tree-reduction over partial aggregates to reduce wall-clock latency and improve cache locality, and (ii) incremental reconstruction that updates partial estimates as subexperiment results arrive, enabling overlap between late execution and early aggregation. Both can be instrumented with the same stage-level logging used in this work and evaluated by shifts in the reconstruction fraction and improvements in speed-up saturation.

Variance-aware scheduling and adaptive shot allocation. The current scheduling treats subexperiments as homogeneous tasks, but cutting produces heterogeneous importance weights and potentially different estimator variances across subexperiments. A variance-aware scheduler could prioritise subexperiments that contribute most to estimator uncertainty, and an adaptive shot allocator could shift shots towards high-variance terms while maintaining an overall error budget. The key systems question is whether such policies reduce total time-to-target-error, not merely time-to-fixed-shot completion; answering this would require logging error estimates (or variance proxies) alongside timing.

Explicit staggering controls and tail-latency mitigation. While our straggler experiments demonstrate sensitivity to tail effects (RQ3), a next step is to incorporate explicit, configurable staggering and speculative execution policies into the runtime and log them as first-class parameters. This would enable a controlled study of queueing behaviour, contention, and tail mitigation under heterogeneous task service times, and would allow stronger causal attribution than straggler injection alone.

Hardware-backed evaluation and network-aware effects. Our current measurements are grounded in simulator-based execution and a thread-based worker pool. Extending the study to hardware-backed execution (or a hybrid of simulators and QPUs) would introduce additional sources of heterogeneity: device queueing, network latency, backend batching policies, and job-level rate limits. These effects can change the balance between execution and reconstruction and may increase the benefits of overlap and distributed reduction. The evaluation methodology in this paper is compatible with such an extension, provided that backend submission/response times and queueing delays are logged.

Broader workload coverage and sensitivity analysis.

Finally, extending the evaluation to additional datasets, ansatz depths, feature maps, and observables would allow a more complete characterisation of when cutting is viable for learning workloads. In particular, sensitivity analysis over circuit depth, shot budgets, and optimiser settings would clarify the boundary at which cutting-induced overheads outweigh feasibility gains, and would enable the construction of predictive performance models grounded in measured stage-level costs.

VII. CONCLUSIONS

We proposed a cut-aware estimator execution pipeline and evaluated it as a staged distributed workload with explicit measurement of overheads and bottlenecks. Our results show that circuit cutting introduces substantial end-to-end overheads (RQ1) and that classical reconstruction is a primary contributor to wall-clock time, limiting achievable speed-up under increased parallelism (RQ2). We further demonstrated that straggler-induced tail effects measurably impact time-to-solution, with sensitivity that depends on whether execution or reconstruction dominates the critical path (RQ3). Despite these systems costs, learning outcomes are preserved in the measured settings, and cutting can alter optimisation trajectories without systematic accuracy degradation (RQ4); robustness is similarly preserved under the logged perturbation protocols, with improvements observed in some configurations (RQ5). Overall, our study indicates that scalable circuit cutting for learning workloads requires treating reconstruction and aggregation as first-class systems problems, not secondary post-processing steps, and motivates optimisation of reconstruction, scheduling, and variance-aware execution to make cutting practical at scale.

REFERENCES

- [1] J. Preskill, “Quantum computing in the nisq era and beyond,” *Quantum*, vol. 2, p. 79, 2018.
- [2] M. Cerezo, A. Arrasmith, R. Babbush, S. C. Benjamin, S. Endo, K. Fujii, J. R. McClean, K. Mitarai, X. Yuan, L. Cincio, and P. J. Coles, “Variational quantum algorithms,” *Nature Reviews Physics*, vol. 3, no. 9, pp. 625–644, 2021.
- [3] S. Endo, Z. Cai, S. C. Benjamin, and X. Yuan, “Hybrid quantum-classical algorithms and quantum error mitigation,” *Journal of the Physical Society of Japan*, vol. 90, no. 3, p. 032001, 2021.
- [4] M. Schuld, V. Bergholm, C. Gogolin, J. Izaac, and N. Killoran, “Evaluating analytic gradients on quantum hardware,” *Physical Review A*, vol. 99, no. 3, p. 032331, 2019.
- [5] K. Temme, S. Bravyi, and J. M. Gambetta, “Error mitigation for short-depth quantum circuits,” *Physical Review Letters*, vol. 119, no. 18, p. 180509, 2017.
- [6] J. Dean and S. Ghemawat, “Mapreduce: Simplified data processing on large clusters,” in *Proceedings of the 6th USENIX Symposium on Operating Systems Design and Implementation (OSDI)*, 2004, pp. 137–150. [Online]. Available: <https://research.google.com/archive/mapreduce-osdi04.pdf>
- [7] M. Zaharia, A. Konwinski, A. D. Joseph, R. Katz, and I. Stoica, “Improving mapreduce performance in heterogeneous environments,” in *Proceedings of the 8th USENIX Symposium on Operating Systems Design and Implementation (OSDI)*, 2008. [Online]. Available: https://www.usenix.org/event/osdi08/tech/full_papers/zaharia/zaharia.pdf
- [8] A. Sergeev and M. Del Balso, “Horovod: fast and easy distributed deep learning in tensorflow,” *arXiv preprint*, 2018.
- [9] T. Peng, A. W. Harrow, M. Ozols, and X. Wu, “Simulating large quantum circuits on a small quantum computer,” *Physical Review Letters*, vol. 125, no. 15, p. 150504, 2020.
- [10] W. Tang, T. Tomesh, M. Suchara, J. Larson, and M. Martonosi, “CutQC: Using small quantum computers for large quantum circuit evaluations,” in *Proceedings of the 26th ACM International Conference on Architectural Support for Programming Languages and Operating Systems (ASPLOS)*, 2021, pp. 473–486.
- [11] C. Piveteau and D. Sutter, “Circuit knitting with classical communication,” *arXiv preprint*, 2022.
- [12] A. W. Harrow and A. Lowe, “Optimal quantum circuit cuts with application to clustered hamiltonian simulation,” *PRX Quantum*, vol. 6, no. 1, p. 010316, 2025.
- [13] A. Lowe *et al.*, “Fast quantum circuit cutting with randomized measurements,” *Quantum*, vol. 7, p. 934, 2023.
- [14] A. Madry, A. Makelov, L. Schmidt, D. Tsipras, and A. Vladu, “Towards deep learning models resistant to adversarial attacks,” in *International Conference on Learning Representations (ICLR)*, 2018. [Online]. Available: <https://openreview.net/forum?id=rJzIBfZAb>
- [15] F. Tramèr, A. Kurakin, N. Papernot, I. Goodfellow, D. Boneh, and P. McDaniel, “Ensemble adversarial training: Attacks and defenses,” in *International Conference on Learning Representations (ICLR)*, 2018. [Online]. Available: <https://openreview.net/forum?id=rkZvSe-RZ>
- [16] P. Moritz, R. Nishihara, S. Wang, A. Tumanov, R. Liaw, E. Liang, M. Elibol, Z. Yang, W. Paul, M. I. Jordan, and I. Stoica, “Ray: A distributed framework for emerging ai applications,” in *Proceedings of the 13th USENIX Symposium on Operating Systems Design and Implementation (OSDI)*, 2018. [Online]. Available: <https://www.usenix.org/system/files/osdi18-moritz.pdf>
- [17] A. Peruzzo, J. McClean, P. Shadbolt, M.-H. Yung, X.-Q. Zhou, P. J. Love, A. Aspuru-Guzik, and J. L. O’Brien, “A variational eigenvalue solver on a photonic quantum processor,” *Nature Communications*, vol. 5, p. 4213, 2014.
- [18] N. Moll, P. Barkoutsos, L. S. Bishop, J. M. Chow, A. Cross, D. J. Egger, S. Filipp, A. Fuhrer, J. M. Gambetta, M. Ganzhorn, A. Kandala *et al.*, “Quantum optimization using variational algorithms on near-term quantum devices,” *Quantum Science and Technology*, vol. 3, no. 3, p. 030503, 2018.
- [19] A. Kandala, A. Mezzacapo, K. Temme, M. Takita, M. Brink, J. M. Chow, and J. M. Gambetta, “Hardware-efficient variational quantum eigensolver for small molecules and quantum magnets,” *Nature*, vol. 549, no. 7671, pp. 242–246, 2017.
- [20] J. Biamonte, P. Wittek, N. Pancotti, P. Rebentrost, N. Wiebe, and S. Lloyd, “Quantum machine learning,” *Nature*, vol. 549, no. 7671, pp. 195–202, 2017.
- [21] K. Mitarai, M. Negoro, M. Kitagawa, and K. Fujii, “Quantum circuit learning,” *Physical Review A*, vol. 98, no. 3, p. 032309, 2018.
- [22] V. Havlíček, A. D. Córcoles, K. Temme, A. W. Harrow, A. Kandala, J. M. Chow, and J. M. Gambetta, “Supervised learning with quantum-enhanced feature spaces,” *Nature*, vol. 567, no. 7747, pp. 209–212, 2019.
- [23] H.-Y. Huang, M. Broughton, M. Mohseni, R. Babbush, S. Boixo, H. Neven, and J. R. McClean, “Power of data in quantum machine learning,” *Nature Communications*, vol. 12, p. 2631, 2021.
- [24] J. R. McClean, S. Boixo, V. N. Smelyanskiy, R. Babbush, and H. Neven, “Barren plateaus in quantum neural network training landscapes,” *Nature Communications*, vol. 9, p. 4812, 2018.
- [25] A. Javadi-Abhari, M. Treinish, K. Krsulich, C. J. Wood, J. Lishman, J. Gacon, S. Martiel, P. D. Nation, L. S. Bishop, A. W. Cross, B. R. Johnson, and J. M. Gambetta, “Quantum computing with qiskit,” *arXiv preprint*, 2024.
- [26] IBM Quantum, “Qiskit primitives api documentation (estimator and sampler).” Online documentation, 2024, accessed 2026-01-14. [Online]. Available: <https://quantum.cloud.ibm.com/docs/api/qiskit/primitives>
- [27] V. Bergholm, J. Izaac, M. Schuld, C. Gogolin, N. Killoran *et al.*, “Pennylane: Automatic differentiation of hybrid quantum-classical computations,” *arXiv preprint*, 2018.
- [28] M. Broughton, G. Verdon, T. McCourt, A. J. Martinez, J. H. Yoo, S. V. Isakov, P. Massey, R. Halavati, M. Y. Niu, A. Zlokapa *et al.*, “TensorFlow Quantum: A software framework for quantum machine learning,” *arXiv preprint*, 2020.
- [29] M. Zaharia, M. Chowdhury, T. Das, A. Dave, J. Ma, M. McCauley, M. J. Franklin, S. Shenker, and I. Stoica, “Resilient distributed datasets: A fault-tolerant abstraction for in-memory cluster computing,” in *Proceedings of the 9th USENIX Symposium on Networked Systems Design and Implementation (NSDI)*, 2012. [Online]. Available: <https://www.usenix.org/system/files/conference/nsdi12/nsdi12-final138.pdf>

- [30] M. Rocklin, “Dask: Parallel computation with blocked algorithms and task scheduling,” in *Proceedings of the 14th Python in Science Conference (SciPy)*, 2015, pp. 126–132. [Online]. Available: <https://proceedings.scipy.org/articles/Majora-7b98e3ed-013.pdf>
- [31] M. Li, D. G. Andersen, J. W. Park, A. J. Smola, A. Ahmed, V. Josifovski, J. Long, E. J. Shekita, and B.-Y. Su, “Scaling distributed machine learning with the parameter server,” in *Proceedings of the 12th USENIX Symposium on Operating Systems Design and Implementation (OSDI)*, 2014, pp. 583–598. [Online]. Available: https://www.usenix.org/system/files/conference/osdi14/osdi14-paper-li_mu.pdf
- [32] Q. Ho, J. Cipar, H. Cui, J. K. Kim, S. Lee, P. B. Gibbons, G. Gibson, G. R. Ganger, and E. P. Xing, “More effective distributed ml via a stale synchronous parallel parameter server,” in *Advances in Neural Information Processing Systems (NeurIPS)*, 2013. [Online]. Available: <https://papers.neurips.cc/paper/4894-more-effective-distributed-ml-via-a-stale-synchronous-parallel-parameter-server.pdf>
- [33] B. Recht, C. Re, S. Wright, and F. Niu, “Hogwild!: A lock-free approach to parallelizing stochastic gradient descent,” in *Advances in Neural Information Processing Systems (NeurIPS)*, 2011. [Online]. Available: <https://proceedings.neurips.cc/paper/2011/file/218a0aef1d1a4be65601cc6ddc1520e-Paper.pdf>
- [34] M. Cho *et al.*, “BlueConnect: Decomposing all-reduce for deep learning on heterogeneous network hierarchy,” in *Proceedings of Machine Learning and Systems (MLSys)*, 2019. [Online]. Available: <https://mlsys.org/Conferences/2019/doc/2019/130.pdf>
- [35] P. Goyal, P. Dollár, R. B. Girshick, P. Noordhuis, L. Wesolowski, A. Kyrola, A. Tulloch, Y. Jia, and K. He, “Accurate, large minibatch sgd: Training imagenet in 1 hour,” *arXiv preprint*, 2017.
- [36] R. D. Blumofe and C. E. Leiserson, “Scheduling multithreaded computations by work stealing,” *Journal of the ACM*, vol. 46, no. 5, pp. 720–748, 1999.
- [37] A. Carrera Vazquez, C. Tornow, D. Ristè, S. Woerner, M. Takita, and D. J. Egger, “Combining quantum processors with real-time classical communication,” *Nature*, vol. 636, pp. 75–79, 2024.
- [38] J. Garrison *et al.*, “Circuit cutting with quantum serverless,” IBM Research (online), 2023. [Online]. Available: <https://research.ibm.com/publications/circuit-cutting-with-quantum-serverless>
- [39] I. Sirdikov *et al.*, “Circuit knitting toolbox and quantum serverless,” IBM Research (online), 2023. [Online]. Available: <https://research.ibm.com/publications/circuit-knitting-toolbox-and-quantum-serverless>
- [40] C. Johnson *et al.*, “Simulating larger quantum circuits with circuit cutting and quantum serverless,” SC 2023 Poster (IBM Research online record), 2023. [Online]. Available: <https://research.ibm.com/publications/simulating-larger-quantum-circuits-with-circuit-cutting-and-quantum-serverless>
- [41] C. Szegedy, W. Zaremba, I. Sutskever, J. Bruna, D. Erhan, I. Goodfellow, and R. Fergus, “Intriguing properties of neural networks,” *arXiv preprint*, 2013.
- [42] I. J. Goodfellow, J. Shlens, and C. Szegedy, “Explaining and harnessing adversarial examples,” in *International Conference on Learning Representations (ICLR)*, 2015. [Online]. Available: <https://arxiv.org/abs/1412.6572>
- [43] Qiskit Contributors, “Qiskit: An open-source framework for quantum computing,” <https://qiskit.org>, 2024, accessed: 2026-01.
- [44] Qiskit Addon Cutting Contributors, “Circuit cutting with qiskit addons,” <https://qiskit.github.io/qiskit-addon-cutting/>, 2024, accessed: 2026-01.
- [45] Qiskit Machine Learning Contributors, “Qiskit machine learning,” <https://qiskit.org/ecosystem/machine-learning/>, 2024, accessed: 2026-01.
- [46] Y. LeCun, L. Bottou, Y. Bengio, and P. Haffner, “Gradient-based learning applied to document recognition,” *Proceedings of the IEEE*, vol. 86, no. 11, pp. 2278–2324, 1998.